*Am J Physiol Renal Physiol* 290: F1103–F1109, 2006.
First published December 20, 2005; doi:10.1152/ajprenal.00245.2005.

# Glycosylation of the osmoresponsive transient receptor potential channel TRPV4 on Asn-651 influences membrane trafficking

**Hongshi Xu,[1,2] Yi Fu,[1,2] Wei Tian,[1,2] and David M. Cohen[1,2]**

[1]*Division of Nephrology and Hypertension, Department of Medicine, Oregon Health and Science University, and the* [2]*Portland Veterans Affairs Medical Center, Portland, Oregon*

Submitted 13 June 2005; accepted in final form 15 December 2005

**Xu, Hongshi, Yi Fu, Wei Tian, and David M. Cohen.** Glycosylation of the osmoresponsive transient receptor potential channel TRPV4 on Asn-651 influences membrane trafficking. *Am J Physiol Renal Physiol* 290: F1103–F1109, 2006. First published December 20, 2005; doi:10.1152/ajprenal.00245.2005.—We identified a consensus N-linked glycosylation motif within the pore-forming loop between the fifth and sixth transmembrane segments of the osmoresponsive transient receptor potential (TRP) channel TRPV4. Mutation of this residue from Asn to Gln (i.e., $TRPV4_{N651Q}$) resulted in loss of a slower migrating band on anti-TRPV4 immunoblots and a marked reduction in lectin-precipitable TRPV4 immunoreactivity. HEK293 cells transiently transfected with the mutant $TRPV4_{N651Q}$ exhibited increased calcium entry in response to hypotonic stress relative to wild-type TRPV4 transfectants. This increase in hypotonicity responsiveness was associated with an increase in plasma membrane targeting of $TRPV4_{N651Q}$ relative to wild-type TRPV4 in both HEK293 and COS-7 cells but had no effect on overall channel abundance in whole cell lysates. Residue N651 of TRPV4 is immediately adjacent to the pore-forming loop. Although glycosylation in this vicinity has not been reported for a TRP channel, the structurally related hexahelical hyperpolarization-activated cyclic nucleotide-gated channel, HCN2, and the voltage-gated potassium channel, human ether-a-go-go-related (HERG), share a nearly identically situated and experimentally confirmed N-linked glycosylation site which promotes rather than limits channel insertion into the plasma membrane. These data point to a potentially conserved structural and functional feature influencing membrane trafficking across diverse members of the voltage-gated-like ion channel superfamily.

cell volume regulation; hypotonicity; ion channel

THE TRANSIENT RECEPTOR potential, or TRP, channels represent a large family of cation channels regulated by diverse afferent inputs; a subset of TRP channels respond to environmental stimuli such as temperature and tonicity (9). TRPV4 [also known as VR-OAC (24), OTRPC4 (42), VRL-2 (13), and TRP12 (53)] is the mammalian homolog of the *C. elegans* osmosensory protein, OSM9 (24, 42). In transfected (24, 42) and native (1, 20) cells in culture, TRPV4 is activated by hypotonic stress; gating by this stimulus may involve arachidonic acid metabolites and/or direct phosphorylation of the channel via Src-family cytoplasmic tyrosine kinases (49, 50, 54). Based in part on its expression in the blood-brain barrier-deficient osmosensing nuclei of the hypothalamus (24), in conjunction with the abnormal water metabolism exhibited by mice harboring targeted deletions of the TRPV4 gene (25, 28), it has been proposed that the channel is instrumental in the regulation of systemic tonicity. TRPV4 also plays a role in volume regulation at the cellular level. In human airway epithelial cells (1) and Chinese hamster ovary (CHO) cells (3), TRPV4 expression was essential for the regulatory volume decrease that followed hypotonic cell swelling.

Although much is known about the pharmacology of TRP channels, far less is understood about their acute or chronic regulation. It was very recently reported that TRPC channels may be regulated by rapid translocation to the plasma membrane (5). Few studies have addressed membrane trafficking in members of the TRPV family. For TRPV1 channels, a SNARE-dependent exocytic mechanism was inferred (29); similar events may take place with members of the TRPC family (7, 39). TRPV2 translocates to the plasma membrane in response to cell activation with peptide growth factor (21); recombinase gene activator (RGA) protein directly interacts with TRPV2 and likely plays a role in this shuttling process (2, 40, 41). The epithelial calcium channel, TRPV5, is reversibly targeted to the plasma membrane, in part, via an interaction with NHERF2, and specifically, the second PDZ domain of this scaffold protein (15, 32); a similar model is likely operative with TRPC4 (27). We earlier noted probable glycosylation of TRPV4 (54). Because glycosylation may also influence trafficking and function of voltage-gated-like ion channels (16), we investigated the role of glycosylation in the function and targeting of TRPV4.

## METHODS

*Cell surface biotinylation and immunoblotting.* For cell surface biotinylation 48 h after transient transfection, HEK293 or COS-7 monolayers were washed three times with ice-cold PBS, incubated with 0.5 mg/ml Sulfo-NHS-LC-Biotin (Pierce Biotechnology, Rockford, IL) for 30 min at 4°C, quenched with 100 mM glycine in ice-cold PBS for 30 min at 4°C, and then washed three times with ice-cold PBS. Monolayers were lysed in lysis buffer [125 mM NaCl, 50 mM Tris, pH 7.5, 0.1% SDS, 0.5% sodium deoxycholate, 1% Nonidet P-40, 1 mM sodium orthovanadate, 1 mM 4-(2-aminoetryl)-benzenesulfonyl fluoride, 1 μg/ml leupeptin, 1 μg/ml aprotinin, 1 μg/ml pepstatin A, 25 mM β-glycerophosphate, 2 mM sodium pyrophosphate] for 30 min at 4°C. The protein concentrations were determined by the Bradford method (Bio-Rad). Forty microliters of ImmunoPure Streptavidin Beads or Neutravidin beads (Pierce Biotechnology) were added to ~3 mg of biotinylated protein and the mixture was incubated at 4°C for 4 h. The beads were washed five times with ice-cold PBS and eluted with 1× SDS sample buffer. The bead-bound proteins were analyzed by Western blot with affinity-purified polyclonal anti-TRPV4 antibody (54). Whole cell lysates (20 μg) were resolved in parallel for immunoblotting where indicated. For cell fractionation studies, membrane and cytosolic fractions were

Address for reprint requests and other correspondence: D. M. Cohen, Mailcode PP262, Oregon Health and Science Univ., 3314 S.W. US Veterans Hospital Rd., Portland, OR 97239 (e-mail: cohend@ohsu.edu).

The costs of publication of this article were defrayed in part by the payment of page charges. The article must therefore be hereby marked "*advertisement*" in accordance with 18 U.S.C. Section 1734 solely to indicate this fact.

prepared via ultracentrifugation as previously reported (44). Immunoblotting was performed with anti-TRPV4, anti-EGFR, and anti-ERK primary antibodies.

*Transient transfection and fura-2 ratiometry.* HEK293 cells were transiently transfected with Lipofectamine PLUS (Life Technologies) in accordance with the manufacturer's directions using 15 μl of PLUS reagent and 30 μl of Lipofectamine and 4–10 μg of plasmid DNA reagent per 100-mm dish of cells. After 48 h, cells were harvested, washed, and resuspended in 10 ml of HBSS (130 mM NaCl, 4.7 mM KCl, 1.25 mM $CaCl_2$, 1.18 mM $MgSO_4$, 5 mM glucose, 15 mM HEPES, pH 7.5) supplemented with 2 μM fura-2-AM and 100 μl of 2% Pluronic F-127 (20% stock solution in DMSO, Molecular Probes, Eugene, OR) per 100 mM dish, and then incubated for 45 min at 37°C. Cells were pelleted at 1,000 *g* for 5 min at 25°C, resuspended with 1–2 ml of HBSS to achieve final concentration of ~ 2–8 × $10^7$ cells/ml, and maintained on ice for 30 min. The suspended, fura-2-loaded cells (50 μl) were assayed for intracellular calcium concentration ($[Ca^{2+}]_i$) at 37°C in a prewarmed, thermostatically controlled cuvette filled with prewarmed (37°C) HBSS (~300 mosmol/kg$H_2O$) or hypotonic HBSS (~150 mosmol/kg$H_2O$) under constant gentle stirring (2-ml final volume) as previously reported (54). Fluorescent emission was monitored at 510 nm and recorded once per second in the presence of alternating excitation at 340 and 380 nm using a Hitachi F-2500 fluorescence spectrophotometer (Hitachi Instruments, Naperville, IL). Calibration of the fura-2 signal was performed as previously described (35) using fura-2·$Ca^{2+}$ dissociation constant of 224 nM (19). For each experiment, data from three separate cuvettes of treated cells were averaged; experiments were repeated at least three times.

*Analysis of glycosylation.* Putative TRPV4 glycosylation sites were sought with the NetNGlyc 1.0 Server utility (6) on the Center for Biological Sequence Analysis Prediction Servers (Technical University of Denmark; http://www.cbs.dtu.dk/services/). $TRPV4_{N651Q}$ was generated from murine TRPV4 cDNA via site-directed mutagenesis using primers mTRPV4-N651Q-5′ (GACGAGGACCAGAGC**CAG**TGCACGGTGCCCACG) and mTRPV4-N651Q-3′ (CGTGGGCACCGTGCA**CTG**GCTCTGGTCCTCGTC), with noncanonical nucleotides shown in bold. For lectin affinity precipitation studies, whole cell lysates prepared as described above were incubated with concanavalin A-agarose beads (Vector Laboratories). Following washing steps, bound proteins were eluted with 1× SDS sample buffer and loaded directly on SDS/PAGE; whole cell lysates were resolved in adjacent lanes for comparison and resultant blots were probed with anti-TRPV4 antibody. Transmembrane segments were predicted using the "DAS" Transmembrane Prediction Server (http://www.sbc.su.se/~miklos/DAS/) and the Dense Alignment Surface algorithm (11). The hexahelical nature of TRPV4, HCN2, and HERG channels (55) was most reliably detected with this algorithm.

*Image processing and statistical analysis.* For quantitation of autoradiograms, exposed films were scanned (Canon LiDE80) and data were reduced using ImageJ (http://rsb.info.nih.gov/ij/; National Institutes of Health) and Excel (Microsoft). For all depicted scans of enhanced chemiluminescence exposures of immunoblots, contrast was improved by decreasing the maximum input level from 255 to ~175 (Adobe PhotoShop CS) to mimic the true appearance of the exposed film. In Fig. 2*A*, a small handdrawn arrow to the left of the upper TRPV4 band in the middle lane was digitally removed to improve the appearance (there was no signal behind the arrow). All experiments were performed a minimum of three times. Significance was assigned to $P < 0.05$ by *t*-test for correlated samples using raw data, or for independent samples using normalized data (VassarStats; http://faculty.vassar.edu/lowry/VassarStats.html). Only pair-wise comparisons were used for this study (i.e., TRPV4 vs. $TRPV4_{N651Q}$).

## RESULTS

We earlier noted that immunoblots of heterologously expressed and natively expressed TRPV4 revealed multiple bands on SDS/PAGE, perhaps consistent with glycosylation. Treatment of cell lysates with endoglycosidase-F resulted in convergence of these bands to a single faster-migrating band (54). We speculated that glycosylation of TRPV4 might play a functional role and, in particular, in the ability of TRPV4 to reach the cell membrane after synthesis. We scanned the predicted murine TRPV4 amino acid sequence for potential N-linked glycosylation motifs using on-line software in the public domain (NetNGlyc 1.0 Server on the CBS Prediction Servers http://www.cbs.dtu.dk/services/NetNGlyc/). Of 38 total Asn residues, five putative N-linked glycosylation motifs (consensus: NX[ST]) were identified at murine TRPV4 residues 201, 207, 651, 784, and 835 (Fig. 1*A*). Only one of these five putative sites, N651, was located in a potential extracellular milieu, in the predicted pore-forming loop spanning residues 637 through 692 of the channel. Importantly, this high-probability N-glycosylation site was also conserved in all species from which TRPV4 has been cloned (Fig. 1*B*).

We used site-directed mutagenesis to mutate this potential N-linked Asn glycosylation site to a Gln residue (i.e., to $TRPV4_{N651Q}$). When whole cell lysates were prepared from HEK293 cells transiently transfected with TRPV4, two immunodetectable TRPV4 species were evident via SDS/PAGE; only the lower, more rapidly migrating band was present in lysates prepared from cells transfected with the mutant $TRPV4_{N651Q}$ (Fig. 2*A*). This was consistent with the pattern we observed when lysates from TRPV4-transfected cells were subjected to endoglycosidase-F treatment (54), suggesting that glycosylation of the channel had largely been eliminated.

Lectins are plant-derived glycoproteins that bind carbohydrate side chains of other proteins with high efficiency and specificity. The lectin concanavalin A binds a-linked mannose, an invariant constituent of N-linked oligosaccharides (26). We used agarose-bound concanavalin A to affinity-precipitate N-

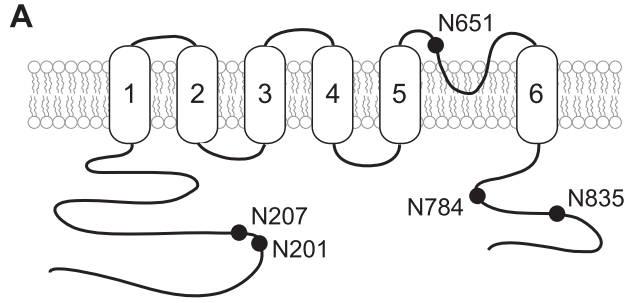


B

| | | |
|---|---|---|
| Human-a | NP_067638 | KVCNEDQTNCTVPTYPS 659 |
| Human-b | NP_671737 | KVCNEDQTNCTVPTYPS 599 |
| Rat | NP_076460 | KVCNEDQSNCTVPSYPA 659 |
| Mouse | NP_071300 | KVCDEDQSNCTVPTYPA 659 |
| Chicken | NP_990023 | ESCSEDHSNCTLPTYPS 645 |

Fig. 1. Structure of potential N-linked glycosylation sites in murine TRPV4. *A*: 6 membrane-spanning domains of TRPV4 are depicted, as are 5 putative N-linked glycosylation motifs (NX[ST]). The single extracellular motif, N651, is in the pore-forming loop between membrane-spanning domains five and six. This site is conserved among all species from which TRPV4 has been cloned (*B*). GenBank accession numbers are shown for TRPV4 predicted amino acid sequence. Of note, numbering of amino acid residues differs from that of mouse for the conceptual translations of human isoform-b and chicken TRPV4.

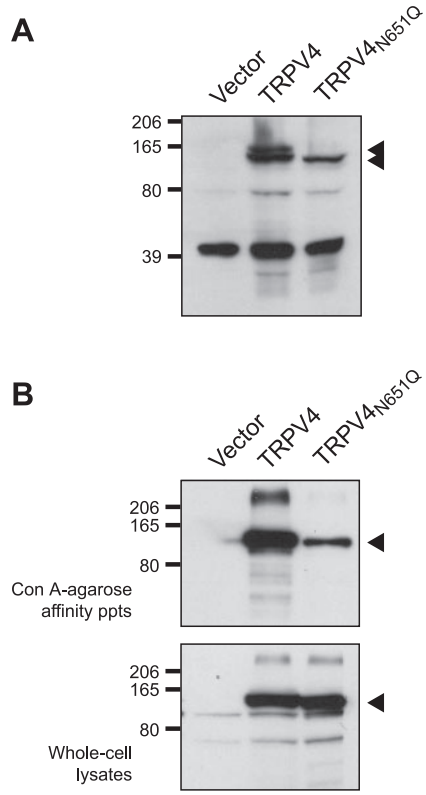


Fig. 2. Point mutation of N651 of murine TRPV4 dramatically decreases glycosylation. *A*: HEK293 cells were transiently transfected with murine TRPV4 cDNA, mutant TRPV4 in which a charge-conserving mutation was made from Asn (N) to Gln (Q) at position 651 (TRPV4$_{N651Q}$), or with empty vector alone. Two TRPV4 species are evident on SDS-PAGE of whole cell lysates prepared from TRPV4-transfected cells; however, only the more rapidly migrating band is evident in the TRPV4$_{N651Q}$-transfected cells. *B*: concanavalin A-agarose affinity precipitates from HEK cells transiently transfected with TRPV4, TRPV4$_{N651Q}$, or empty vector alone. Far less mutant TRPV4 than wild-type TRPV4 was precipitated by the lectin-bound beads (*top*), even though expression was roughly equivalent in the whole cell lysates (*bottom*).

glycosylated proteins from HEK293 cells that had been transiently transfected with wild-type TRPV4, TRPV4$_{N651Q}$, or empty vector alone. Although equivalent amounts of TRPV4 and TRPV4$_{N651Q}$ were expressed in the transfectants, there was a dramatic reduction in the amount of TRPV4$_{N651Q}$ bound by the lectin-agarose beads, relative to TRPV4 (Fig. 2*B*). Taken together, these data in Fig. 2 indicated that we had successfully eliminated nearly all of the TRPV4 glycosylation through mutation of this single residue.

We anticipated that mutagenesis of this site might produce a hypofunctioning channel. Unexpectedly, on transient expression in HEK293 cells, TRPV4$_{N651Q}$ exhibited greater responsiveness to hypotonicity. Specifically, calcium influx following hypotonic stress in fura-2-loaded TRPV4$_{N651Q}$ transient transfectants exceeded that of cells transfected with the wild-type TRPV4 (Fig. 3*A*). In cells transfected with vector alone, there was only minimal response to hypotonicity. Peak calcium influx occurred at ~75 s of exposure to hypotonicity; at this time point, the increment in intracellular calcium was significantly greater in the TRPV4$_{N651Q}$ transfectants than in the TRPV4 transfectants (Fig. 3*B*). Of note, in these studies, as in our earlier observations with TRPV4 in this model (54), calcium transients in the presence of either wild-type TRPV4 or TRPV4$_{N651Q}$ were completely dependent on the presence of extracellular calcium (data not shown). We also tested the effect of more modest hypotonic stress (10 rather than 50%). Of note, when this more modest degree of hypotonic stress was applied, maximal calcium entry occurred at ~100 s following application of the stimulus rather than at 75 s and this time point was used for comparison. In addition, owing to the more modest effect, fura-2 ratio in response to hypotonicity in the absence of extracellular calcium was determined for each of the transfectants at this time point and this value was subtracted. Therefore, extracellular calcium-dependent calcium entry in response to 10% hypotonicity is reported (Fig. 3*C*). In five of five experiments, a stronger signal was observed in both TRPV4-transfected and in TRPV4$_{N651Q}$-transfected cells than in vector-transfected cells; in four of five experiments, the effect of TRPV4$_{N651Q}$ exceeded that of wild-type TRPV4 (data not shown). However, interassay variability resulted in only the TRPV4 transfectants achieving clear statistical significance relative to vector (Fig. 3*C*); there was a trend for the effect of TRPV4$_{N651Q}$ to exceed that of wild-type TRPV4 and vector alone. These data in general were supportive of those derived from transfectants exposed to more profound hypotonic stress. For clarity, we focused on the effect of the major hypotonic challenge.

Because defects in glycosylation may influence trafficking of proteins to the plasma membrane, and trafficking of voltage-gated ion channels in particular (30, 33), we next investigated whether the wild-type and mutant channels were expressed at the cell surface with equal efficiency. Anti-TRPV4 immunofluorescence confocal microscopy was performed using HEK and COS-7 cells that had been transiently transfected with either TRPV4 of TRPV4$_{N651Q}$. The intercell variability within each transfectant was high (i.e., >2-fold) making direct comparison between wild-type and mutant TRPV4 infeasible (data not shown); selection of truly "representative" fields for comparison between transfectants was not possible. We isolated membrane fractions via differential centrifugation and noted increased TRPV4$_{N651Q}$ expression relative to that of wild-type TRPV4 (data not shown).

To quantify cell surface expression of wild-type and glycosylation-defective TRPV4, we performed cell surface biotinylation experiments. HEK293 cells were transiently transfected with either wild-type TRPV4 or TRPV4$_{N651Q}$ and subjected to cell surface biotinylation; labeled channels were affinity-precipitated with avidin-agarose and resolved via SDS/PAGE. Although there was no difference in the levels of expression in whole cell lysates (Fig. 4, *A* and *B*), the mutant was expressed at a significantly higher level at the cell surface (Fig. 4, *A* and *C*). These data indicated that the hyperresponsiveness of the TRPV4$_{N651Q}$ transfectants was likely a consequence of increased plasma membrane expression of the channel. We confirmed these observations in the COS-7 cell line (Fig. 4*A*). Importantly, we do not assert that there is acute recruitment of either wild-type or glycosylation-deficient TRPV4 to the cell surface in response to anisotonicity, per se. Rather, the functional changes between the wild-type and mutant channel were interpreted to correlate with their differing expression levels.

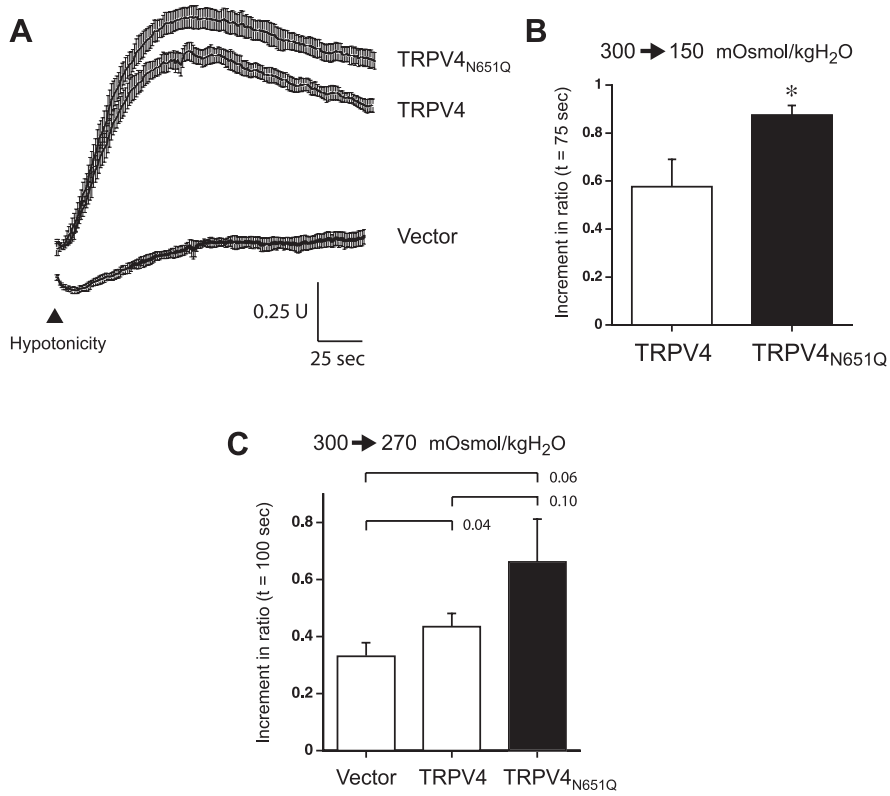


Fig. 3. Cells transfected with $TRPV4_{N651Q}$ are hyperresponsive to hypotonic stress. *A*: HEK293 cells transiently transfected with murine TRPV4, $TRPV4_{N651Q}$, or empty vector were loaded with fura-2 and subjected to hypotonic stress (arrowhead). Fura-2 ratio (in arbitrary units; U) as an index of intracellular calcium concentration is depicted as a function of time (s). *B*: increment in fura 2 ratio (relative to basal fura-2 ratio) in response to hypotonic stress (300 mosmol/kg$H_2O$ → 150 mosmol/kg$H_2O$) at $t = 75$ s is shown for TRPV4 and $TRPV4_{N651Q}$ transfectants ($n = 3$; means ± SE). For comparison, the increment in fura-2 ratio in cells transfected with empty vector alone was ~0.2 (data not shown). *C*: increment in fura-2 ratio in response to a more subtle hypotonic stress (300 mosmol/kg$H_2O$ → 270 mosmol/kg$H_2O$) at $t = 100$ s in HEK cells transiently transfected with empty vector alone or with wild-type TRPV4 or $TRPV4_{N651Q}$. For these experiments, the time point of 100 s was selected because it coincided with the maximal response to this lesser osmotic challenge. In addition, for these data alone, the contribution of hypotonic stress to the intracellular calcium transient in the absence of extracellular calcium (calculated from experiments performed in parallel) was subtracted. (The contribution of this effect to the data in *B* was negligible.) *P* values for the indicated comparisons are shown above the bars.

## DISCUSSION

We earlier noted probable glycosylation of the osmosensing TRPV channel, TRPV4 (54), but were unaware of its functional significance. Here, we describe glycosylation of TRPV4 and map the site of N-linked oligosaccharide attachment to the pore-forming loop via a combination of mutagenesis, immunoblotting, and functional studies. Mutation of this glycosylation motif increases trafficking of TRPV4 to the plasma membrane and consequently increases net calcium entry in response to TRPV4 agonist (i.e., hypotonicity).

Little is known about the role of glycosylation in the function of other TRP channels. TRPC3 and TRPC6 undergo mono- and diglycosylation, respectively (14, 48), but these sites on the first and second extracellular loops bear no evident relationship to the pore-forming loop. These motifs are functionally significant; however, elimination of the glycosylation site unique to TRPC6 and retention of the glycosylation site shared by both converts the tightly receptor-regulated TRPC6 to the constitutively active TRPC3 phenotype (14).

While this manuscript was in review, Chang et al. (8) reported that, similar to what we observed with TRPV4, TRPV5 expression in the plasma membrane is upregulated when its solitary glycosylation site is mutated. These data bolster our unexpected observation concerning the role of glycosylation in the regulation of TRPV4. This group went on to demonstrate that dynamic deglycosylation of TRPV5 may occur at the membrane and is likely mediated by the intrinsic glucuronidase activity of the anti-aging hormone (23), *klotho*, acting via the circulation or tubule lumen (8). A similar mechanism may be operative in the regulation of TRPV4.

Glycosylation has been reported to influence trafficking and/or function of other voltage-gated-like ion channels. This protein superfamily includes the TRP, two pore segment (TPC), voltage-gated sodium ($Na_V$), voltage-gated calcium ($Ca_V$), hyperpolarization-activated cyclic nucleotide gated (HCN), cyclic nucleotide-gated (CNG), voltage-gated potassium ($K_V$), two-pore potassium ($K_{2p}$), calcium-activated potassium ($K_{Ca}$), and inwardly rectifying potassium ($K_{ir}$) channel families (55). Of these, the architecture of the $K_V$, HCN, CNG, and $K_{Ca}$ channels most closely resembles that of the TRP channels, with six membrane-spanning domains and a pore-forming loop between helices five and six. Interestingly, the most abundant evidence for a functional role for glycosylation comes from this subgroup; two members, human ether-a-go-go-related gene (HERG) channel and the HCN2 cyclic nucleotide-gated channel, share N-linked glycosylation sites in the pore-forming loop that influence membrane trafficking and are potentially analogous to that of TRPV4 (Fig. 5). In HERG channels (also known as $K_V11.1$), mutagenesis of this glycosylation site causes aberrant targeting (18, 33); a naturally occurring human mutation appears to be linked to a variant of the "long QT syndrome" and its attendant predisposition to potentially lethal cardiac dysrhythmias (37). In HCN2, a channel mutated for the putative glycosylation site similarly failed to traffic to the plasma membrane (30). Unlike these members of the voltage-gated-like chanome (55), TRPV4 membrane trafficking is downregulated rather than facilitated by glycosylation.

Other "hexahelical" members of the voltage-gated-like ion channel superfamily are influenced by glycosylation. The prototypical voltage-gated potassium channel, Shaker ($K_V1.1$), is regulated by glycosylation at the level of both function and membrane trafficking (12, 22, 43, 51, 52, 57), although not all reports arrived at this conclusion (36). Other closely related

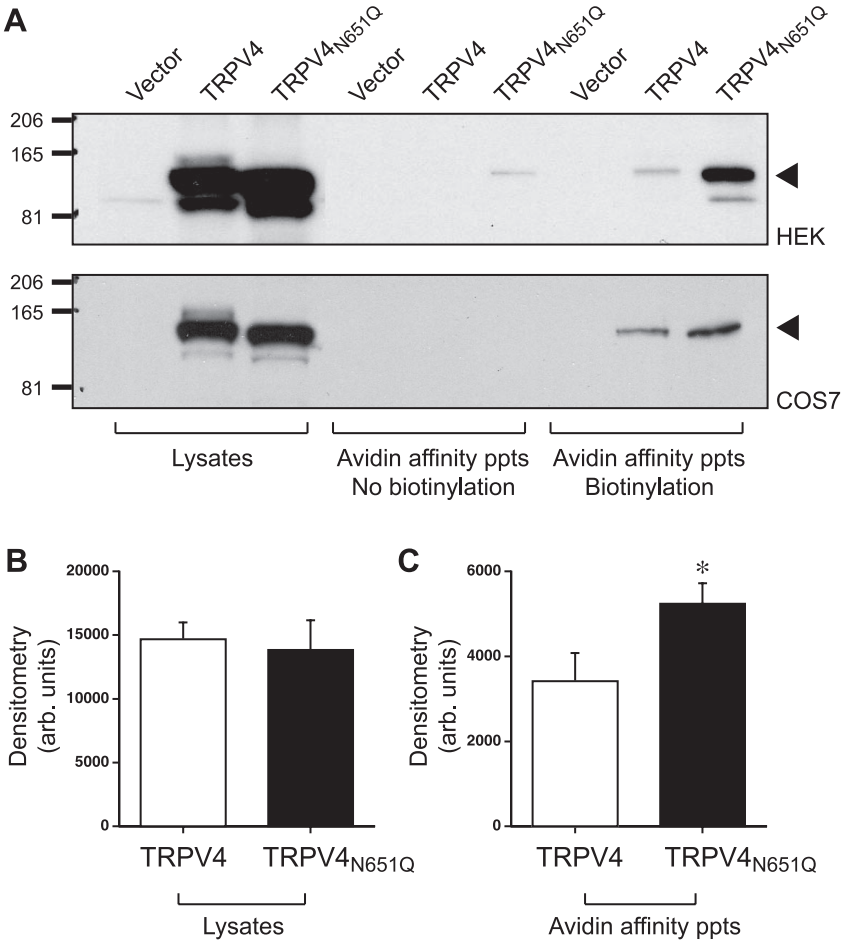


Fig. 4. $TRPV4_{N651Q}$ exhibits increased cell surface expression. *A*: HEK and COS7 cells were transiently transfected with TRPV4 or with $TRPV4_{N651Q}$ and cells were either subjected to cell-surface biotinylation or sham treatment ("No biotinylation"); whole cell lysates and avidin-affinity precipitates of whole cell lysates were prepared from each group and resolved via SDS-PAGE and then immunoblotted with anti-TRPV4. Quantitation of the relative abundance of TRPV4 and $TRPV4_{N651Q}$ in whole cell lysates from HEK cells (*B*) and in avidin-affinity precipitates from surface-biotinylated HEK cells (*C*) is shown.

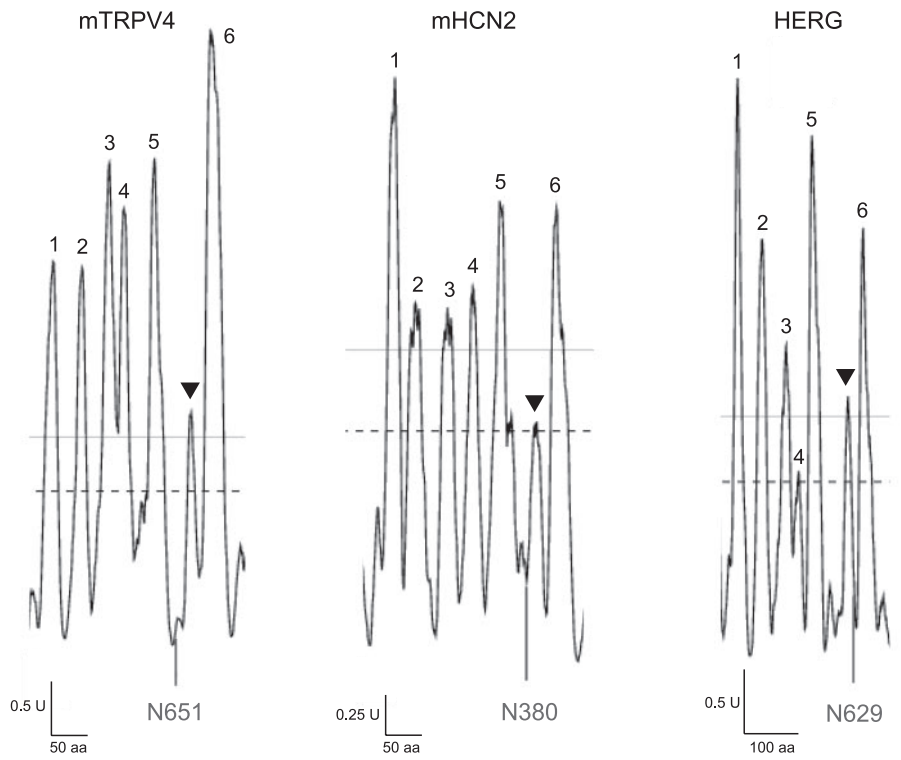


Fig. 5. Glycosylation sites adjacent to the pore-forming domain in multiple voltage-gated cation channels. Transmembrane segments were predicted for murine TRPV4 (mTRPV4), murine HCN2, and HERG (human $K_v11.1$) using the "DAS" Transmembrane Prediction Server (http://www.sbc.su.se/~miklos/DAS/) and the Dense Alignment Surface algorithm (11). Only the regions of each protein corresponding to the six membrane-spanning helices (S1-S6) are shown (i.e., residues ~465–720 for mTRPV4, ~185–440 for mHCN2, and ~385–685 for HERG) and are numbered 1 through 6; the pore-forming hairpin is indicated by the arrowhead. Locations of the glycosylation sites are shown in red [present data and (30, 33)]; in each case, the indicated site has been experimentally confirmed and appears to be the only high-abundance glycosylation site in the protein. For each panel, horizontal scale depicts relative amino acid number and vertical scale represents DAS profile score (an index of hydrophobicity expressed in arbitrary units). The horizontal gray line and dashed line indicate "loose" and "strict" cutoff criteria, respectively, for membrane-spanning domains.

members of the $K_V1.x$ subfamily may be similarly regulated (38, 52), as are $K_V4$ (47) and the nonvoltage-gated minK channel (a subunit of $K_V7.1$) (17, 47).

In addition to the examples above, voltage-gated-like ion channels lacking the hexahelical architecture may also be regulated by glycosylation (10, 31, 34). Much like the case with $K_V11.1$, a naturally occurring point mutation of a putative glycosylation site in the human cardiac voltage-gated sodium channel, $Na_V1.5$, was associated with a form of the long QT syndrome (16, 46, 56). Elimination of glycosylation in the skeletal muscle variant, $Na_V1.4$, and in the related $Na_V1.9$, through mutagenesis or enzymatic action, similarly altered channel functional properties (4, 45, 56).

With respect to TRPV4, it is possible that there are additional glycosylation sites. Although mutation of the N651 site abolished the slower-migrating species on SDS/PAGE, it did not eradicate all lectin-precipitable TRPV4. The other high-probability sites for N-linked glycosylation are all intracellular and hence represent unlikely targets. O-linked glycosylation occurs on Ser or Thr residues, or on hydroxylysines in collagen (26); however, no high probability O-glycosylation sites were identified in TRPV4 (data not shown). Because mutation of a single residue resulted in elimination of almost all of lectin binding (i.e., >80%; Fig. 2*B*), there is unlikely to be a remaining "stoichiometric" glycosylation site. We believe the most likely explanation for the residual binding of $TRPV4_{N651Q}$ to the lectin-conjugated beads is nonspecific adherence to the solid phase itself; we were, however, unable to obtain unconjugated beads of this identical chemistry from the manufacturer to test this hypothesis. It is also noteworthy that, in some experiments, the migration of the $TRPV4_{N651Q}$ mutant was perhaps slightly faster than that of the presumed nonglycosylated (i.e., faster migrating) form of wild-type TRPV4. It is possible that this wild-type TRPV4 species is not completely devoid of glycosylation; we were unable to exclude this possibility in our initial observation (54).

TRPV4 influences the regulatory volume decrease that follows acute hypotonic cell swelling in in vitro models (1, 3). We have not specifically investigated the role of the N651 residue of TRPV4 in this process. Because mutation of this residue increases trafficking of this channel to the membrane and therefore increases acute calcium entry in the setting of hypotonic stress, we speculate that its regulatory volume decrease response is preserved and potentially even enhanced. But the differing levels of cell surface expression between the wild-type and mutant channels preclude the design of rigorously controlled experiments.

In summary, there is a single high-probability N-linked glycosylation site in TRPV4 that faces the extracellular milieu and is phylogenetically conserved. From a structural perspective, this site is immediately adjacent to the hydrophobic "hairpin" of the pore-forming loop. Mutation of this residue to Gln abolishes TRPV4-associated glycosylation as assessed via mobility on SDS/PAGE, and by lectin affinity precipitation. This mutation is also associated with enhanced trafficking of the channel to the plasma membrane as evidenced by functional studies and cell surface biotinylation. Two other members of the voltage-gated cation channel superfamily, HCN2 and HERG ($K_V11.1$), also have putative N-linked glycosylation sites adjacent to the pore-forming loop; mutagenizing the responsible Asn residue in these channels, however, abolishes channel activity and/or membrane trafficking. These data point to a potentially conserved structural and functional feature among diverse members of the voltage-gated-like ion channel superfamily that plays an important role in channel trafficking to the plasma membrane.

## GRANTS

This work was supported by the National Institutes of Health, American Heart Association, and Department of Veterans Affairs.

## REFERENCES

1. **Arniges M, Vazquez E, Fernandez-Fernandez JM, and Valverde MA.** Swelling-activated $Ca^{2+}$ entry via TRPV4 channel is defective in cystic fibrosis airway epithelia. *J Biol Chem* 279: 54062–54068, 2004.
2. **Barnhill JC, Stokes AJ, Koblan-Huberson M, Shimoda LM, Muraguchi A, Adra CN, and Turner H.** RGA protein associates with a TRPV ion channel during biosynthesis and trafficking. *J Cell Biochem* 91: 808–820, 2004.
3. **Becker D, Blase C, Bereiter-Hahn J, and Jendrach M.** TRPV4 exhibits a functional role in cell-volume regulation. *J Cell Sci* 118: 2435–2440, 2005.
4. **Bennett E, Urcan MS, Tinkle SS, Koszowski AG, and Levinson SR.** Contribution of sialic acid to the voltage dependence of sodium channel gating. A possible electrostatic mechanism. *J Gen Physiol* 109: 327–343, 1997.
5. **Bezzerides VJ, Ramsey IS, Kotecha S, Greka A, and Clapham DE.** Rapid vesicular translocation and insertion of TRP channels. *Nat Cell Biol* 6: 709–720, 2004.
6. **Blom N, Sicheritz-Ponten T, Gupta R, Gammeltoft S, and Brunak S.** Prediction of posttranslational glycosylation and phosphorylation of proteins from the amino acid sequence. *Proteomics* 4: 1633–1649, 2004.
7. **Cayouette S, Lussier MP, Mathieu EL, Bousquet SM, and Boulay G.** Exocytotic insertion of TRPC6 channel into the plasma membrane upon Gq protein-coupled receptor activation. *J Biol Chem* 279: 7241–7246, 2004.
8. **Chang Q, Hoefs S, van der Kemp AW, Topala CN, Bindels RJ, and Hoenderop JG.** The β-glucuronidase klotho hydrolyzes and activates the TRPV5 channel. *Science* 310: 490–493, 2005.
9. **Clapham DE.** TRP channels as cellular sensors. *Nature* 426: 517–524, 2003.
10. **Cronin NB, O'Reilly A, Duclohier H, and Wallace BA.** Effects of deglycosylation of sodium channels on their structure and function. *Biochemistry* 44: 441–449, 2005.
11. **Cserzo M, Wallin E, Simon I, von Heijne G, and Elofsson A.** Prediction of transmembrane α-helices in prokaryotic membrane proteins: the dense alignment surface method. *Protein Eng* 10: 673–676, 1997.
12. **De Souza NF and Simon SM.** Glycosylation affects the rate of traffic of the Shaker potassium channel through the secretory pathway. *Biochemistry* 41: 11351–11361, 2002.
13. **Delany NS, Hurle M, Facer P, Alnadaf T, Plumpton C, Kinghorn I, See CG, Costigan M, Anand P, Woolf CJ, Crowther D, Sanseau P, and Tate SN.** Identification and characterization of a novel human vanilloid receptor-like protein, VRL-2. *Physiol Genomics* 4: 165–174, 2001.
14. **Dietrich A, Mederos y Schnitzler M, Emmel J, Kalwa H, Hofmann T, and Gudermann T.** N-linked protein glycosylation is a major determinant for basal TRPC3 and TRPC6 channel activity. *J Biol Chem* 278: 47842–47852, 2003.
15. **Embark HM, Setiawan I, Poppendieck S, van de Graaf SF, Boehmer C, Palmada M, Wieder T, Gerstberger R, Cohen P, Yun CC, Bindels RJ, and Lang F.** Regulation of the epithelial $Ca^{2+}$ channel TRPV5 by the NHE regulating factor NHERF2 and the serum and glucocorticoid inducible kinase isoforms SGK1 and SGK3 expressed in *Xenopus* oocytes. *Cell Physiol Biochem* 14: 203–212, 2004.
16. **Fozzard HA and Kyle JW.** Do defects in ion channel glycosylation set the stage for lethal cardiac arrhythmias? *Sci STKE* 2002: PE19, 2002.
17. **Freeman LC, Lippold JJ, and Mitchell KE.** Glycosylation influences gating and pH sensitivity of I(sK). *J Membr Biol* 177: 65–79, 2000.
18. **Gong Q, Anderson CL, January CT, and Zhou Z.** Role of glycosylation in cell surface expression and stability of HERG potassium channels. *Am J Physiol Heart Circ Physiol* 283: H77–H84, 2002.

19. **Grynkiewicz G, Poenie M, and Tsien RY.** A new generation of $Ca^{2+}$ indicators with greatly improved fluorescence properties. *J Biol Chem* 260: 3440–3450, 1985.
20. **Jia Y, Wang X, Varty L, Rizzo CA, Yang R, Correll CC, Phelps PT, Egan RW, and Hey JA.** Functional TRPV4 channels are expressed in human airway smooth muscle cells. *Am J Physiol Lung Cell Mol Physiol* 287: L272–L278, 2004.
21. **Kanzaki M, Zhang YQ, Mashima H, Li L, Shibata H, and Kojima I.** Translocation of a calcium-permeable cation channel induced by insulin-like growth factor-I. *Nat Cell Biol* 1: 165–170, 1999.
22. **Khanna R, Myers MP, Laine M, and Papazian DM.** Glycosylation increases potassium channel stability and surface expression in mammalian cells. *J Biol Chem* 276: 34028–34034, 2001.
23. **Kuro-o M, Matsumura Y, Aizawa H, Kawaguchi H, Suga T, Utsugi T, Ohyama Y, Kurabayashi M, Kaname T, Kume E, Iwasaki H, Iida A, Shiraki-Iida T, Nishikawa S, Nagai R, and Nabeshima Y.** Mutation of the mouse klotho gene leads to a syndrome resembling ageing. *Nature* 390: 45–51, 1997.
24. **Liedtke W, Choe Y, Marti-Renom MA, Bell AM, Denis CS, Sali A, Hudspeth AJ, Friedman JM, and Heller S.** Vanilloid receptor-related osmotically activated channel (VR-OAC), a candidate vertebrate osmoreceptor. *Cell* 103: 525–535, 2000.
25. **Liedtke W and Friedman JM.** Abnormal osmotic regulation in trpv4−/− mice. *Proc Natl Acad Sci USA* 100: 13698–13703, 2003.
26. **Lodish HF, Berk A, Zipursky SL, Matsudaira P, Baltimore D, and Darnell JE Jr.** Protein sorting: organelle biogenesis and protein secretion. In: *Molecular Cell Biology*. New York: W. H. Freeman, 1999, p. 712–722.
27. **Mery L, Strauss B, Dufour JF, Krause KH, and Hoth M.** The PDZ-interacting domain of TRPC4 controls its localization and surface expression in HEK293 cells. *J Cell Sci* 115: 3497–3508, 2002.
28. **Mizuno A, Matsumoto N, Imai M, and Suzuki M.** Impaired osmotic sensation in mice lacking TRPV4. *Am J Physiol Cell Physiol* 285: C96–C101, 2003.
29. **Morenilla-Palao C, Planells-Cases R, Garcia-Sanz N, and Ferrer-Montiel A.** Regulated exocytosis contributes to protein kinase C potentiation of vanilloid receptor activity. *J Biol Chem* 279: 25665–25672, 2004.
30. **Much B, Wahl-Schott C, Zong X, Schneider A, Baumann L, Moosmang S, Ludwig A, and Biel M.** Role of subunit heteromerization and N-linked glycosylation in the formation of functional hyperpolarization-activated cyclic nucleotide-gated channels. *J Biol Chem* 278: 43781–43786, 2003.
31. **Pabon A, Chan KW, Sui JL, Wu X, Logothetis DE, and Thornhill WB.** Glycosylation of GIRK1 at Asn119 and ROMK1 at Asn117 has different consequences in potassium channel function. *J Biol Chem* 275: 30677–30682, 2000.
32. **Palmada M, Poppendieck S, Embark HM, van de Graaf SF, Boehmer C, Bindels RJ, and Lang F.** Requirement of PDZ domains for the stimulation of the epithelial Ca2+ channel TRPV5 by the NHE regulating factor NHERF2 and the serum and glucocorticoid inducible kinase SGK1. *Cell Physiol Biochem* 15: 175–182, 2005.
33. **Petrecca K, Atanasiu R, Akhavan A, and Shrier A.** N-linked glycosylation sites determine HERG channel surface membrane expression. *J Physiol* 515: 41–48, 1999.
34. **Recio-Pinto E, Thornhill WB, Duch DS, Levinson SR, and Urban BW.** Neuraminidase treatment modifies the function of electroplax sodium channels in planar lipid bilayers. *Neuron* 5: 675–684, 1990.
35. **Roullet JB, Luft UC, Xue H, Chapman J, Bychkov R, Roullet CM, Luft FC, Haller H, and McCarron DA.** Farnesol inhibits L-type $Ca^{2+}$ channels in vascular smooth muscle cells. *J Biol Chem* 272: 32240–32246, 1997.
36. **Santacruz-Toloza L, Huang Y, John SA, and Papazian DM.** Glycosylation of shaker potassium channel protein in insect cell culture and in Xenopus oocytes. *Biochemistry* 33: 5607–5613, 1994.
37. **Satler CA, Vesely MR, Duggal P, Ginsburg GS, and Beggs AH.** Multiple different missense mutations in the pore region of HERG in patients with long QT syndrome. *Hum Genet* 102: 265–272, 1998.
38. **Shi G and Trimmer JS.** Differential asparagine-linked glycosylation of voltage-gated $K^+$ channels in mammalian brain and in transfected cells. *J Membr Biol* 168: 265–273, 1999.
39. **Singh BB, Lockwich TP, Bandyopadhyay BC, Liu X, Bollimuntha S, Brazer SC, Combs C, Das S, Leenders AG, Sheng ZH, Knepper MA, Ambudkar SV, and Ambudkar IS.** VAMP2-dependent exocytosis regulates plasma membrane insertion of TRPC3 channels and contributes to agonist-stimulated $Ca^{2+}$ influx. *Mol Cell* 15: 635–646, 2004.
40. **Stokes AJ, Shimoda LM, Koblan-Huberson M, Adra CN, and Turner H.** A TRPV2-PKA signaling module for transduction of physical stimuli in mast cells. *J Exp Med* 200: 137–147, 2004.
41. **Stokes AJ, Wakano C, Del Carmen KA, Koblan-Huberson M, and Turner H.** Formation of a physiological complex between TRPV2 and RGA protein promotes cell surface expression of TRPV2. *J Cell Biochem* 94: 669–683, 2005.
42. **Strotmann R, Harteneck C, Nunnenmacher K, Schultz G, and Plant TD.** OTRPC4, a nonselective cation channel that confers sensitivity to extracellular osmolarity. *Nat Cell Biol* 2: 695–702, 2000.
43. **Thornhill WB, Wu MB, Jiang X, Wu X, Morgan PT, and Margiotta JF.** Expression of Kv1.1 delayed rectifier potassium channels in Lec mutant Chinese hamster ovary cell lines reveals a role for sialidation in channel function. *J Biol Chem* 271: 19093–19098, 1996.
44. **Traub O, Monia BP, Dean NM, and Berk BC.** PKC- is required for mechano-sensitive activation of ERK1/2 in endothelial cells. *J Biol Chem* 272: 31251–31257, 1997.
45. **Tyrrell L, Renganathan M, Dib-Hajj SD, and Waxman SG.** Glycosylation alters steady-state inactivation of sodium channel Nav1.9/NaN in dorsal root ganglion neurons and is developmentally regulated. *J Neurosci* 21: 9629–9637, 2001.
46. **Ufret-Vincenty CA, Baro DJ, Lederer WJ, Rockman HA, Quinones LE, and Santana LF.** Role of sodium channel deglycosylation in the genesis of cardiac arrhythmias in heart failure. *J Biol Chem* 276: 28197–28203, 2001.
47. **Ufret-Vincenty CA, Baro DJ, and Santana LF.** Differential contribution of sialic acid to the function of repolarizing $K^+$ currents in ventricular myocytes. *Am J Physiol Cell Physiol* 281: C464–C474, 2001.
48. **Vannier B, Zhu X, Brown D, and Birnbaumer L.** The membrane topology of human transient receptor potential 3 as inferred from glycosylation-scanning mutagenesis and epitope immunocytochemistry. *J Biol Chem* 273: 8675–8679, 1998.
49. **Vriens J, Watanabe H, Janssens A, Droogmans G, Voets T, and Nilius B.** Cell swelling, heat, and chemical agonists use distinct pathways for the activation of the cation channel TRPV4. *Proc Natl Acad Sci USA* 101: 396–401, 2004.
50. **Watanabe H, Vriens J, Prenen J, Droogmans G, Voets T, and Nilius B.** Anandamide and arachidonic acid use epoxyeicosatrienoic acids to activate TRPV4 channels. *Nature* 424: 434–438, 2003.
51. **Watanabe I, Wang HG, Sutachan JJ, Zhu J, Recio-Pinto E, and Thornhill WB.** Glycosylation affects rat Kv1.1 potassium channel gating by a combined surface potential and cooperative subunit interaction mechanism. *J Physiol* 550: 51–66, 2003.
52. **Watanabe I, Zhu J, Recio-Pinto E, and Thornhill WB.** Glycosylation affects the protein stability and cell surface expression of Kv1.4 but not Kv11 potassium channels. A pore region determinant dictates the effect of glycosylation on trafficking. *J Biol Chem* 279: 8879–8885, 2004.
53. **Wissenbach U, Bodding M, Freichel M, and Flockerzi V.** Trp12, a novel Trp related protein from kidney. *FEBS Lett* 485: 127–134, 2000.
54. **Xu H, Zhao H, Tian W, Yoshida K, Roullet JB, and Cohen DM.** Regulation of a transient receptor potential (TRP) channel by tyrosine phosphorylation. SRC family kinase-dependent tyrosine phosphorylation of TRPV4 on TYR-253 mediates its response to hypotonic stress. *J Biol Chem* 278: 11520–11527, 2003.
55. **Yu FH and Catterall WA.** The VGL-chanome: a protein superfamily specialized for electrical signaling and ionic homeostasis. *Sci STKE 2004*: re15, 2004.
56. **Zhang Y, Hartmann HA, and Satin J.** Glycosylation influences voltage-dependent gating of cardiac and skeletal muscle sodium channels. *J Membr Biol* 171: 195–207, 1999.
57. **Zhu J, Watanabe I, Poholek A, Koss M, Gomez B, Yan C, Recio-Pinto E, and Thornhill WB.** Allowed N-glycosylation sites on the Kv1.2 potassium channel S1–S2 linker: implications for linker secondary structure and the glycosylation effect on channel function. *Biochem J* 375: 769–775, 2003.